Pharmaceutical Research, Vol. 23, No. 11, November 2006 (© 2006)
DOI: 10.1007/s11095-006-9078-2

Research Paper

Polymorph Farming of *Acetaminophen* and *Sulfathiazole* on a Chip

Tu Lee,[1,2,3] Shi Ting Hung,[1] and Chung Shin Kuo[1]

Received January 4, 2006; accepted June 5, 2006; published online September 13, 2006

Purpose. The aim of this paper is to understand at a given temperature (1) the role of template films, the droplet volume of a saturated *sulfathiazole aqueous* solution and the solvent on polymorph screening of *sulfathiazole on a silicon wafer*, and (2) the effect of template films on the acetaminophen crystal face at the template-crystal interface.

Materials and Methods. *Template Effect:* Spun cast template films of non-annealed chitosan and annealed chitosan at 140°C on silicon wafers were prepared. A 0.01-cm^3 saturated sulfathiazole aqueous solution droplets were deposited on both kinds of chitosan film. Sulfathiazole crystals were produced on those films by evaporation at 25°C.

Volume Effect: Different droplet volumes of a saturated sulfathiazole aqueous solution ranging from 0.01 to 0.14 to 2.7 cm^3 were deposited on non-annealed chitosan films. Sulfathiazole crystals were generated on those films by evaporation at 25°C.

Solvent Effect: 0.01 cm^3 saturated sulfathiazole methanol solution droplets were deposited on non-annealed chitosan films and sulfathiazole crystals were formed on those films by evaporation at 25°C.

The formation pathways of different *sulfathiazole* crystal polymorphs of the above mentioned effects were analyzed and verified by systematic studies.

Template-crystal Interfacial Study: Millimeter-sized acetaminophen crystals were successfully grown on non-annealed chlorosulfonated poly(ethylene) (PE-Chl) and chitosan template films by cooling the saturated acetaminophen aqueous solution from 50 to 25°C in which those template films were immersed. The bonding energies for specific carbons collected by electron spectroscopy for chemical analysis (ESCA) at the acetaminophen crystal surface, together with the molecular interactions between acetaminophen and PE-Chl and between acetaminophen and chitosan in separately prepared solid dispersion film samples detected by Fourier transformed infrared (FTIR) spectroscopy, proved to be useful for identifying the crystal face of acetaminophen essential for its specific intermolecular interactions at the template-crystal interface.

Results. Thermodynamically metastable sulfathiazole Form I crystals were reproducibly obtained on the non-annealed chitosan films whereas the stable sulfathiazole Form III crystals were repeatedly formed on the annealed chitosan films. Droplet volumes and solvents were also found responsible for the polymorphic outcome of sulfathiazole in the kinetically driven area of two overlapping metastable zones from two competing polymorphs of Form I and Form III. Thermodynamically stable sulfathiazole Form III crystals were formed on the non-annealed chitosan films instead when the droplet volumes of a saturated sulfathiazole aqueous solution were increased from 0.01 to 0.14 cm^3 and 2.7 cm^3. When the solvent was changed from water to methanol, the thermodynamically stable sulfathiazole Form III crystals were again observed on the non-annealed chitosan films even from the 0.01 cm^3 saturated sulfathiazole methanol solution droplets.

Conclusions. Template surfaces were thought to provide specific functional groups to either change the energy barrier for the nuclei formation of the thermodynamically metastable Form I or alter the droplet contact angle and the droplet surface area which was related to the droplet evaporation time. The evaporation time determines the amount of time available for the polymorphic transformation from Form I to Form III. Apparently, droplet volumes could also determine the amount of time needed to reach supersaturation and the amount of time available for a polymorphic transformation from Form I to Form III. In addition, the molecular conformation and viscosity of solvents such as methanol might alter the original nucleation kinetics in water and lead to a more rapid polymorphic transformation from Form I to Form III. Template films of PE-Chl and chitosan were found to be critical for determining the

[1] Department of Chemical and Materials Engineering, National Central University, 300 Jhong-Da Rd, Jhong-Li 320, Taiwan, Republic of China.
[2] Institute of Materials Science and Engineering, National Central University, 300 Jhong-Da Rd, Jhong-Li 320, Taiwan, Republic of China.
[3] To whom correspondence should be addressed. (e-mail: tulee@cc.ncu.edu.tw)

face of a millimeter-sized acetaminophen crystal at the template-crystal interface. The idea of performing polymorph screening on the template film deposited on *a chip* has opened up a new doorway to examine the roles of: (1) various kinds of drug carrier in the form of a template film, (2) the droplet volume of a saturated solution, and (3) the type of solvent used, in polymorphic control. Growing millimeter-sized crystals directly on the chip of template has also provided a convenient technology enabling platform for examining the crystal-template interface by solid-state characterization techniques such as ESCA.

KEY WORDS: acetaminophen; chip; chitosan; chlorosulfonated poly(ethylene); ESCA; FTIR; polymorph farming; sulfathiazole.

INTRODUCTION

Self-assembly and self-recognition of molecules, atoms or ions are often precisely packed in a number of different long-range orders through intermolecular forces. Each of this order at the sub-nanometer level in solid-state is termed a crystal polymorph. Since each polymorph is a unique material with its own physicochemical properties (1), the discovery and selection of a desired polymorph are essential in food (2), explosives (3), optoelectronics (4), agricultural (5) and ceramics (6) industry. They are especially so in the pharmaceutical industry. Polymorph screening is highly important for the active pharmaceutical ingredients (APIs) not only for their physicochemical aspects (7) but also for their legal considerations (8).

Recently, four automated platforms based on miniaturizing the conventional re-crystallization methods have been reported. These methods are: (1) an array of glass test tubes in aluminum blocks (9), (2) polymer heteronuclei in the 96-well polypropylene plate (10), (3) an array of square metallic gold islands with self-assembled monolayers (SAMs) of lateral dimensions ranging from 25 to 725 μm as nucleation sites (11), and (4) an array of microdroplets of many different carrier/drug formulations directly deposited on the surface of the attenuated total reflection (ATR) crystal (12).

With the use of an *in situ* optical and Raman microscopy, methods (1) and (2) have apparently removed the time-consuming crystal isolation-characterization step in the chain of events of crystallization—crystal isolation-characterization. However, the design of these two enabling platforms does not allow solid-state characterizations such as electron spectroscopy for chemical analysis (ESCA) to understand the molecular recognitions at the template-crystal interface. The lengthy preparation of combinatorial conditions of different solvents and polymer heteronuclei has also prolonged the crystallization process. As for method (3), the key drawback lies on the cost and the limited varieties of commercially available SAMs with different functionalities. Although many foreign compounds other than SAMs can serve as nucleation sites in pharmaceutical product development, such as the drug carriers in formulations, these compounds cannot be readily grafted on the metallic islands in method (3). Unlike method (3), method (4) has taken the drug carriers into a consideration. Its sample deposition and spectroscopic imaging are fast, but small drug crystals dispersed in the drug/carrier microdroplets are difficult to isolate for some other characterizations such as PXRD, DSC, microindentation and ESCA.

Therefore, a new strategy that enables: (1) a universal fabrication step dedicated only to the preparation of combinatorial conditions, and (2) a more general platform for many other kinds of physicochemical analysis, should effectively shorten the time-consuming chain of activities in polymorph screening. Inspired by the microarrays in drug discovery (13) and built on the ideas of templated crystallization (10,11, 14–20), our strategy is to grow crystal polymorphs on templates of soft materials, such as drug carriers and polymers, which can be conveniently deposited on silicon wafers by spin coating.

Here we report our current attempts in this area, including our own strategy called, Polymorph Farming on a Chip. If desired, this technology enabling platform can be easily coupled with *microscopy and spectroscopy such as* optical microscopy (OM) and Fourier transformed infrared (FTIR) spectroscopy, which allows a thorough search for polymorphs under the influences of: (1) drug-carrier surface, (2) droplet volume of a saturated solution, and (3) solvent. At the same time, this strategy minimizes *the amount of sample* and the sample preparation time for crystallization, isolation and characterization activities, in which many methods are lacking (9–12).

Sulfathiazole, an early antibiotic agent (Fig. 1a) and acetaminophen, an analgesic drug (Fig. 1b) were chosen for this study mainly because of their commercial values and their well-characterized polymorphs by FTIR (21,22), DSC (23,24) and PXRD (23,25). As for the interfacial study between the template and the crystal face, acetaminophen is a better candidate than sulfathiazole due to the ease of growing large-sized acetaminophen crystals in the solution. PE-Chl (Fig. 1c) and chitosan (Fig. 1d) were the two chosen soft materials for template preparation. PE-Chl is a polymer reported to be capable of inducing the thermodynamically unstable Form II needles of acetaminophen in water by evaporation (10). Chitosan is a polysaccharide of many applications in pharmaceutical system as a drug carrier (26), biomimetic process (27) and optical wave guide (28).

MATERIALS AND METHODS

Chemicals

Sulfathiazole (Form III) white crystalline powders ($C_9H_9N_3O_2S_2$, M.W. = 255.31, m.p. = 201–204°C, 98%) were purchased from Fluka (Buchs SG, Switzerland). Acetaminophen (Form I) white crystalline powders ($CH_3CONHC_6H_4OH$, M.W. = 151.17, m.p. = 169–172°C, 98%) and chitosan flakes ($C_{12}H_{24}N_2O_9$, medium molecular weight) were bought from Aldrich (Milwaukee, WI, U.S.A.). Chlorosulfonated poly(ethylene) chunks (43% Cl, 1.1% S (as SO_2Cl), Average M_w = 195,000) were purchased from Acros Organics (Geel, Belgium). Anhydrous potassium bromide powders (KBr, F.W. = 119.01, spectrograde) were received from Perkin Elmer (Garfield, NJ, U.S.A.). Acetic acid glacial

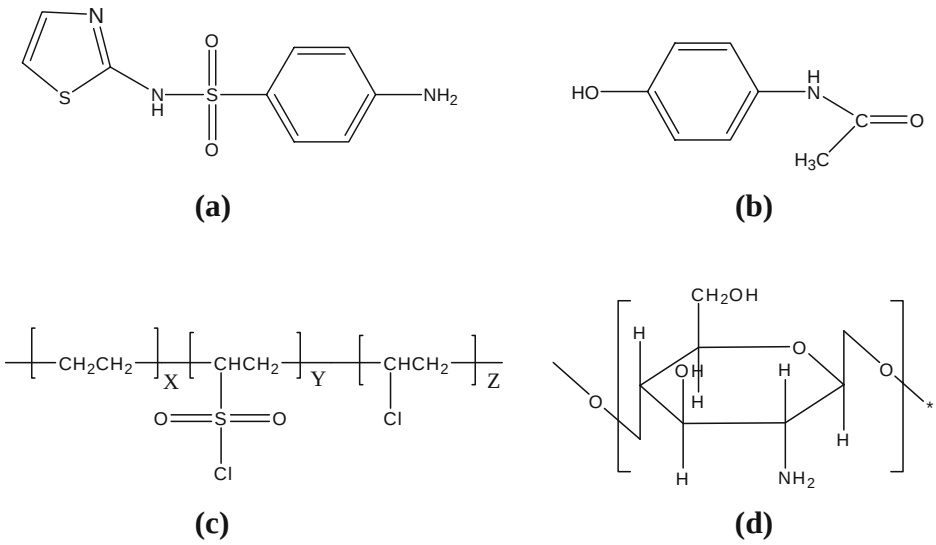

Fig. 1. Molecular structures of (a) sulfathiazole, (b) acetaminophen, (c) chlorosulfonated poly(ethylene) (PE-Chl), and (d) chitosan.

(CH_3COOH, M.W. = 60.05) was obtained from Scharlau Chemie S.A. (Barcelona, Spain). Methanol (CH_3OH, M.W. = 32.04, b.p. = 64.7°C), toluene ($C_6H_5CH_3$, M.W. = 92.14, b.p. = 110.6°C), 2-propanol (IPA) ($(CH_3)_2CHOH$, M.W. = 60.10, b.p. = 82.4°C) and tetrahydrofuran (THF) (C_4H_8O, M.W. = 72.11, b.p. = 65–67°C) were obtained from Tedia (Fairfield, OH, U.S.A). De-ionized water (DI water) was used in all experiments.

Instrumentations

Power X-Ray Diffraction (PXRD)

The crystallinity of template films was examined by powder X-ray diffraction (PXRD). PXRD diffractographs were collected on Bruker D8 Advance (Karlsruhe, Germany). The source of PXRD was Cu–Kα radiation (1.542 angstrom) and the diffractometer was operated at 40 keV and 41 mA. The X-ray was passed through a 1 mm incident slit and the signal was passed through a 1 mm detector slit, a nickel filter, and another 0.1 mm detector slit. The detector type was scintillation counter. The scanning rate was 1.2° 2θ/min with chopper increment of 0.02° 2θ and the angular range was from 5° to 35° 2θ under room temperature. The template film samples were fixed on a sample holder by a double-sided tape. Template film preparation steps were contained under the section of Template Preparation in detail.

Atomic Force Microscopy (AFM)

AFM was utilized to examine the integrity, the morphology and the topography of template film surfaces, which shed light on (1) the surface modification of chitosan films before and after annealing, (2) the surface differences between chitosan and PE-Chl non-annealed template films, and (3) whether the polymers from the template films leached out into the crystal growing media before and after crystallization. AFM experiments were performed with an SPA400/SPI3800N (Seiko Instruments Inc., Tokyo, Japan). A silicon micro-cantilever, coated with aluminum (NO. 10371, Si-DF20, Seiko Instruments Inc., Tokyo, Japan; 200 mm in length, resonant frequency of 127 kHz, spring constant of 12 N/m) was used in the dynamic force mode (DFM) at a frequency of 1.0 Hz. The maximum scanning area was 20 × 20 μm, but all samples were scanned at 1 × 1 μm by tapping mode. The average analysis time was 5 min per sample. All experiments were conducted under room temperature.

Optical Microscopy (OM)

Crystal habits and contact angles were examined and measured by an Olympus SZII Zoom Stereo Microscope (Olympus, Tokyo, Japan) equipped with a Sony SSC-DC 50A digital color video camera (Sony Corporation, Tokyo, Japan).

Fourier Transform Infrared (FTIR) Spectroscopy

Transmission FTIR spectroscopy was used to determine for (1) polymorphism, (2) intermolecular interactions, and (3) possible polymer contamination. FTIR spectra were recorded on a Perkin Elmer Spectrum One spectrometer (Perkin Elmer Instruments LLC, Shelton, CT, U.S.A.).

For polymorphism determination, 1 to 2 mg of harvested powder samples of sulfathiazole were well mixed with about 48 mg KBr powders and isostatically pressed into a disk by a pressure of 7 tons. The disk was scanned with a scan number of 8 from 450 to 4,000 cm^{-1} having a resolution of 2 cm^{-1}.

To identify and simulate possible intermolecular interactions at the template–crystal interface, thin films of (1) non-annealed chitosan, (2) annealed chitosan, (3) non-annealed PE-Chl, (4) chitosan–sulfathiazole solid dispersion, (5) chitosan–acetaminophen solid dispersion, and (6) PE-Chl-acetaminophen solid dispersion, were all analyzed and compared directly by transmission FTIR with a scan number of 8 from 450 to 4,000 cm^{-1} having a resolution of 2 cm^{-1}. All thin films were sandwiched between two round aluminum foil disks with a diameter of 1.2 cm having a center hole of 2 mm in diameter and mounted to a FTIR sample holder. KBr pressing disk method could not be used here because of the elastic nature of

chitosan and PE-Chl. Thin film preparation steps were described in detail under the section of Molecular Interactions Study.

To ensure that chitosan and PE-Chl from the template films did not leach out into the crystal growing media and affected the crystal growth, 1 to 2 g of chitosan flakes and PE-Chl chunks were immersed in 20 ml of water for two days for cleansing. The clean chitosan flakes and PE-Chl chunks were immersed in 20 ml of water again for two days. About 10 ml of filtered supernatant was collected in which 100 mg of KBr was co-dissolved. The resultant solution was then vacuum oven dried to solid powders at 50°C. The powders were isostatically pressed into a disk by a pressure of 7 tons. The disk was scanned with a scan number of 8 from 450 to 4,000 cm^{-1} having a resolution of 2 cm^{-1}.

Differential Scanning Calorimetry (DSC)

DSC was used to cross-examine polymorphism of sulfathiazole and acetaminophen crystals which were gently dislodged from the template films by a piece of wax paper. Thermal analytical data of 3 to 5 mg of samples in perforated aluminum sample pans (25 μl) were collected on a Perkin Elmer DSC-7 calorimeter (Perkin Elmer Instruments LLC, Shelton, CT, U.S.A.) with a temperature scanning rate of 10°C/min from 50 to 200°C under a constant nitrogen 99.990% purge. The instrument was calibrated with indium 99.999% (Perkin Elmer Instruments LLC, Shelton, CT, U.S.A.).

Electron Spectroscopy for Chemical Analysis (ESCA)

ESCA VG-Scientific sigma probe manufactured by Thermo (East Grinstead, U.K.) with a probe size of 400 μm was used to determine the surface structures of acetaminophen crystal faces (about 1 mm in width) that were in contact with templates of soft materials. Three acetaminophen crystals plucked from each template film of PE-Chl and chitosan *were turned upside down* and mounted on a copper conductive tape (Prod. No. 16074, TED Pella Inc., California, USA) in such a way that faces originally in contact with templates were facing upward for ESCA analyses. The edge of each crystal was then carefully grounded with a carbon conductive tape (Prod. No. 16073, TED Pella Inc., California, USA). Crystals in a preparation chamber were firstly vacuumed down to 10^{-8} Torr before transferred to an analytical chamber of 10^{-10} Torr. A Super Dynamic II CCD camera (Panasonic, Tokyo, Japan) was used to locate the area of analysis. The spectra were collected on a monochromatic spectrometer (Thermo Electron Corporation, Minneapolis, MN, U.S.A.) using an Al Kα source (600 W, 1486.6 eV). The angles of incidence and reflection of the X-ray made with the crystal surface were 45°. The survey scan ranged from 0 to 1,400.00 eV in 1.00 eV step. The higher resolution utility scan ranging from 275 to 295 eV in a step of 0.1 eV was used to determine the bonding energy of the C_{1S} for hydrocarbons at 285 eV and the one for C = O at 288 eV.

Experiments

The flow diagram in Fig. 2 summaries the systematic studies in our present paper. To investigate the individual role of template, droplet volume, and solvent on polymorphism of sulfathiazole: (1) *non-annealed and annealed* chitosan thin films were prepared (*Template Preparation*), (2) polymorphs were induced on those template films (*Template*

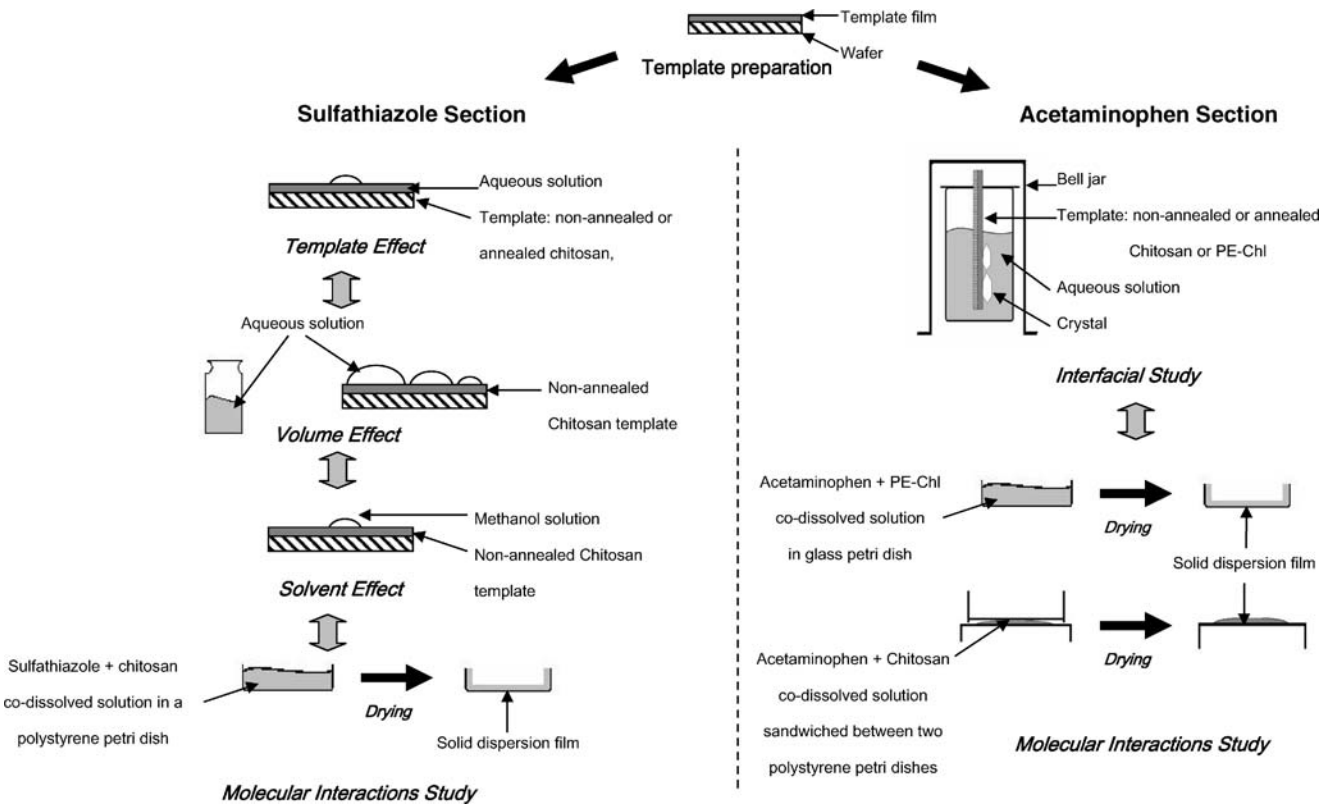

Fig. 2. The flowchart of experiments in the present study.

Effect), (3) polymorphs were formed in different volumes of *saturated sulfathiazole aqueous solution* (*Volume Effect*), (4) polymorphs were grown in *saturated sulfathiazole methanol solution* (*Solvent Effect*), and (5) solid dispersed sulfathiazole–chitosan thin films were prepared (*Molecular Interactions Study*). As for determining the crystal face in contact with the template surface at the molecular level: (1) millimeter-sized acetaminophens were *attempted* to grow on *non-annealed and annealed* PE-Chl and chitosan thin films (*Interfacial Study*). ESCA was used to examine *the binding energies for carbon* at the crystal face, and (2) solid dispersed acetaminophen–PE-Chl thin films and acetaminophen–chitosan thin films were prepared (*Molecular Interactions Study*). FTIR was employed to identify interactions among different kinds of molecule.

Template Preparation

Silicon wafers were roughened in a mixed solution of HCl:H_2O with a volume ratio of 1:5 for 30 min at 50°C, rinsed by a copious amount of IPA and dried by nitrogen. Water-insoluble films of PE-Chl and chitosan were obtained by spin casting the 1% (w/w) PE-Chl–toluene solution and the 1% (w/w) solution of chitosan in a 1% (w/w) acetic aqueous solution on silicon wafers at 800 and 1,500 rpm for 30 s, respectively, by a spin coater (General Space Enterprise Co. Ltd., Taipei, Taiwan). A thicker film for crystallinity determination by PXRD can be obtained by simply pouring the polymer solution into a petri dish.

For non-annealed template film preparation, all films were only needed to be vacuum dried at 50°C overnight. But for the annealed template films, all films were required to be vacuum dried at 140°C overnight.

Sulfathiazole Section

Template Effect. Multiple drops of the saturated sulfathiazole aqueous solution (0.47 mg/ml at 25°C) with a volume of 0.01 cm^3 each were introduced on *both non-annealed and annealed chitosan template films* by a pipette. Crystallization was induced by water evaporation at 25°C. Water evaporation rate of the droplets was constantly monitored as the total weight loss of the system *versus* time by a weighing balance and a stopwatch.

Volume Effect. Droplets with volumes of about 0.01, 0.14 and 2.7 cm^3 of the saturated sulfathiazole aqueous solution (0.47 mg/ml at 25°C) were deposited on three separate *non-annealed* chitosan template films by a pipette. Crystallization was induced by water evaporation at 25°C. To study the extreme case in volume effect, sulfathiazole crystals were also obtained from the evaporation of a 20-ml saturated aqueous solution of sulfathiazole in a scintillation vial. Water evaporation rate was constantly monitored for all experiments as the total weight loss of the system *versus* time by a weighing balance and a stopwatch.

Solvent Effect. Droplets with a volume of 0.01 cm^3 of the saturated sulfathiazole methanol solution (10 mg/ml at 25°C) were deposited on the chitosan template film by a pipette. Crystallization was induced by methanol evaporation at 25°C. Methanol evaporation rate was constantly monitored in the experiment as the total weight loss of the system *versus* time by a weighing balance and a stopwatch.

Molecular Interactions Study. To identify the interactions among sulfathiazole and chitosan molecules a solid dispersed film was made. 0.007 g of sulfathiazole and 0.007 g of chitosan were co-dissolved in a 100 ml of 1% (w/w) acetic aqueous solution. Twenty milliliters of the co-dissolved solution was cast on a glass petri dish. The solid dispersion film was vacuum dried at 50°C overnight before subjected to a transmission FTIR analysis.

Acetaminophen Section

Interfacial Study. A saturated acetaminophen aqueous solution with a solubility of 50 mg/ml at 50°C was prepared. *Non-annealed and annealed* template films of PE-Chl and chitosan with a dimension of about 3 × 5 cm were placed vertically in a 500-ml beaker filled with a saturated acetaminophen aqueous solution at 50°C. To ensure good mixing, the acetaminophen solution was constantly stirred by a magnetic spin-bar. The experiment was covered by an inverted 1-l bell jar at all times to minimize the lost of solvent. Crystallization was induced by cooling to 25°C. Crystallization was completed in 5 to 6 h. Crystals grown on the template surfaces were vacuum dried together with the template films at 45°C overnight before the ESCA analysis.

Molecular Interactions Study. To identify the interactions among acetaminophen and PE-Chl molecules, and among acetaminophen and chitosan molecules, a solid dispersed film of each kind was made: (1) 0.5 g of acetaminophen and 0.5 g of PE-Chl were co-dissolved in 50 ml of THF. The co-dissolved solution was cast on a glass petri dish. (2) 0.5 g of acetaminophen and 0.5 g of chitosan were co-dissolved in a 50 ml of 1% (w/w) acetic aqueous solution. The co-dissolved solution was then sandwiched between two polystyrene petri dishes. Both kinds of solid dispersion film were vacuum dried at 40°C overnight before subjected to a transmission FTIR analysis.

RESULTS AND DISCUSSION

In the Template Effect section, sulfathiazole grown on the *non-annealed chitosan template film* from the evaporation of 0.01 cm^3 droplets of saturated sulfathiazole aqueous solution at 25°C were 500 μm long rod-like crystals by optical microscopy. The contact angle of the droplet was 50° and it took 360 min to complete evaporation. The crystal polymorph was verified to be the thermodynamically unstable Form I (29) by FTIR. Characteristic bands for Form I (21) at 1,200 and 1,308 cm^{-1} were detected (Fig. 3). On the other hand, 300 μm long needle thermodynamically stable sulfathiazole Form III crystals (29) with characteristic bands (21) at 1,322 and 1,424 cm^{-1} (Fig. 3) were obtained from the evaporation of 0.01 cm^3 saturated sulfathiazole aqueous solution droplets on the annealed chitosan template at 25°C. The contact angle of the droplet was 70° and the water evaporation took 600 min to finish.

From the FTIR spectrum of a compressed disk prepared by co-drying the aqueous supernatant of chitosan and KBr, no chitosan characteristic bands were observed. This indicated that chitosan was insoluble in water and did not leach out from the template film into the droplets of a saturated sulfathiazole aqueous solution. Therefore, the template effect on polymorphic control was a surface phenomenon.

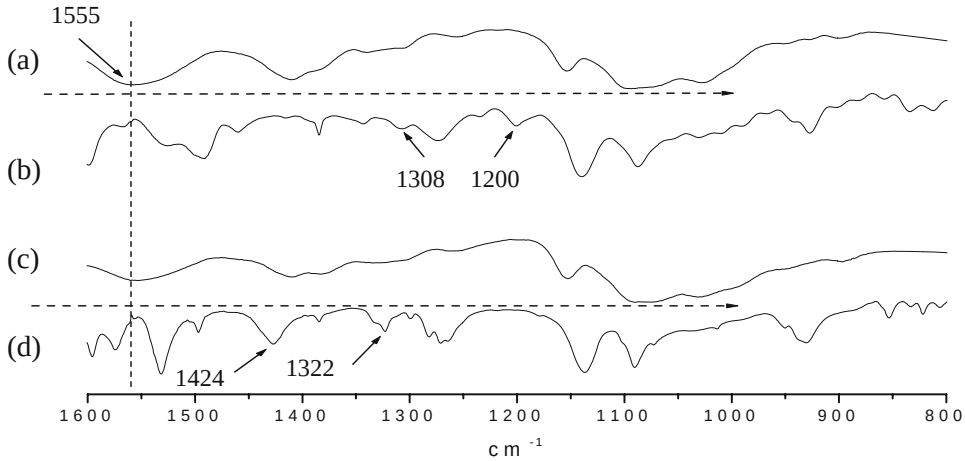

Fig. 3. FTIR spectra of (a) non-annealed chitosan template film, (b) sulfathiazole Form I crystals, (c) annealed chitosan template film, and (d) sulfathiazole Form III crystals.

PXRD showed that both non-annealed and annealed chitosan template films were amorphous. The AFM images (Fig. 4) showed no detectable differences in the morphology and topography of non-annealed and annealed chitosan template films at the nanometer scale. However, the surface stereochemical make-ups could have been different at the molecular level. These subtle differences were perhaps caused by the conformational change (30) of amide and amine groups as indicated by the decrease in the area and shift in the FTIR amide peak position around 1,555 cm^{-1} (Fig. 3a and c). This suggests that a significant rearrangement of bond structure may be taking place within the acetamide and/or amine bond regions (30). The end result of this might then affect the orientation, the spacing and the distribution of the specific chitosan functional groups responsible for the polymorphic control of sulfathiazole at the template film surface.

The stereochemical make-ups at the template film surface could either change the free energy required to form the critical size of an assembly of molecules for a thermodynamically metastable polymorph (1) or alter the droplet contact angle and droplet surface area through intermolecular forces such as hydrogen bondings. Based on the contact angle measurements, the non-annealed chitosan template film was more hydrophilic than the annealed chitosan template film and the droplet surface area ratio between the two 0.01 cm^3 droplets was about 1.4. Since the droplet area could influence the evaporation time, the evaporation time ratio of the two droplets were experimentally determined to be about 1.8.

Functional groups in chitosan that might be participating in the polymorphic control of sulfathiazole were the OH and NH_2 groups. As illustrated by the FTIR spectrum of sulfathiazole–chitosan solid dispersion film sample (Fig. 5), the molecular interactions between the OH and NH_2 groups in chitosan and the S = O group in sulfathiazole were observed. The 3,400 cm^{-1} stretch assigned to OH and NH_2 groups in chitosan was increased in width while the 1,323 cm^{-1} asymmetric stretch assigned to S = O in sulfathiazole was lowered in intensity relative to other adjacent peaks. Assignments of IR bands of sulfathiazole and chitosan are shown in Table I (31–33).

To ferret out other possible influences on polymorph farming on a chip, different droplet volumes of a saturated sulfathiazole aqueous solution ranging from 0.01 to 0.14 to 2.7 cm^3 and finally to a 20 ml volume were prepared in the Volume Effect section. As the droplet volume of a saturated sulfathiazole aqueous solution increased, the polymorph of sulfathiazole grown by the water evaporation method at 25°C transformed from the thermodynamically unstable Form I to the stable Form III as shown by the FTIR spectra (Fig. 6) During polymorphic transformation, characteristic bands for Form I (21) at 1,200 and 1,308 cm^{-1} (Fig. 6b) disappeared

Table I. IR Assignments of Acetaminophen, Chlorosulfonated Polyethylene and Chitosan

Wave Numbers (cm^{-1})	Functional Groups	References
Sulfathiazole		
3,279	$–NH_2$ (sym stretch)	(31)
3,320	$–NH_2$ (asym stretch)	(31)
1,136	$C–SO_2–N$ (sym stretch)	(31)
1,323	$C–SO_2–N$ (asym stretch)	(31)
1,531	C = N	(31)
631	C–S	(31)
Chitosan		
3,450–3,100	–OH (stretch)	(33)
3,450–3,250	$–NH_2$ (stretch)	(34)
2,990–2,850	Aliphatic C–H (stretch)	(33)
1,650–1,590	$–NH_2$ (bending)	(34)
1,460–1,200	C–O–C (stretch)	(34)
Acetaminophen		
3,325	N–H (stretch)	(44)
3,163	–OH (stretch)	(44)
1,653	C = O (stretch)	(44)
1,564	N–H (in-plane bending)	(44)
1,610, 1,506, 1,441	Aromatic ring	(44)
1,327	O–H (bending)	(44)
1,259–1,227	C–O and/or C–N (amide stretch)	(44)
Chlorosulphonated Polyethylene (PE-Chl)		
2,924	$–CH_3$, $–CH_2–$, >CH– (stretch)	(45)
2,854	$–CH_3$, $–CH_2–$, >CH– (stretch)	(45)
1,480–1,440	$–CH_2–$ (bending)	(45)
1,367	$–SO_2Cl–$ (asym stretch)	(45)
1,260	$–CH_2–$ (bending)	(45)
1,163	$–SO_2Cl–$ (sym stretch)	(45)

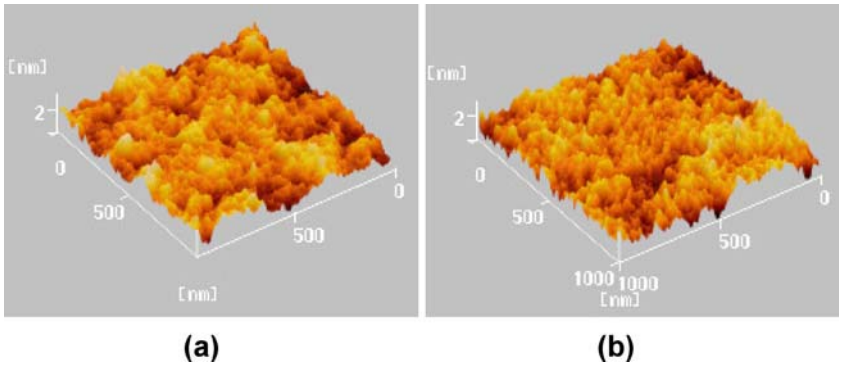

Fig. 4. AFM images of (a) non-annealed chitosan template film, and (b) annealed chitosan template film.

and new characteristic bands for Form III (21) at 850, 882, 950 and 1,020 cm^{-1} appeared (Fig. 6e).

Although Form I was induced kinetically at first in 0.01 cm^3 droplets of a saturated sulfathiazole aqueous solution by the non-annealed chitosan template film, if the droplet volume had become larger, as water in the droplet of a saturated sulfathiazole aqueous solution evaporated, homogeneous nucleation of thermodynamically stable Form III could have had time to occur in the solution phase of the droplet. This might explain the co-existence of both Form I and Form III in a 0.14 cm^3 droplet volume (Fig. 6c) with an evaporation time of 540 min. Since a relatively large volume of water of 10 ml took even longer to dry up (about 30 days), this would allow plenty of time for the polymorphic transformation to complete by Osward ripening (34) from Form I to Form III as demonstrated in Fig. 6e.

Another possible factor for polymorphic control was explored in the Solvent Effect section. A more volatile solvent such as methanol was used to replace water and yet crystals grown from the evaporative crystallization of 0.01 cm^3 droplets of a saturated sulfathiazole methanol solution on the non-annealed chitosan template film at 25°C were verified to be a thermodynamically stable Form III by FTIR (21,31) (Fig. 7). Interestingly, using a non-annealed chitosan template, a small droplet volume of 0.01 cm^3 and a short evaporation time of 80 min for methanol solution, did not warrant the formation of Form I sulfathiazole crystals. One plausible explanation is that the structural similarities between the conformation in methanol solution and in the Form III crystal might have made the nucleation kinetics of Form III favorable (29). In addition, the viscosity of methanol is about half of the value of water of 0.9×10^{-3} Pa·s at 25°C (35). This would definitely increase the molecules mobility, which might lead to a more rapid transformation of Form I to Form III than the one in water (36). The physical meaning of the 20-fold higher solubility of sulfathiazole in methanol than in water at 25°C could be taken into account by re-scaling all the numbers originally on the concentration axis of the solubility curve for

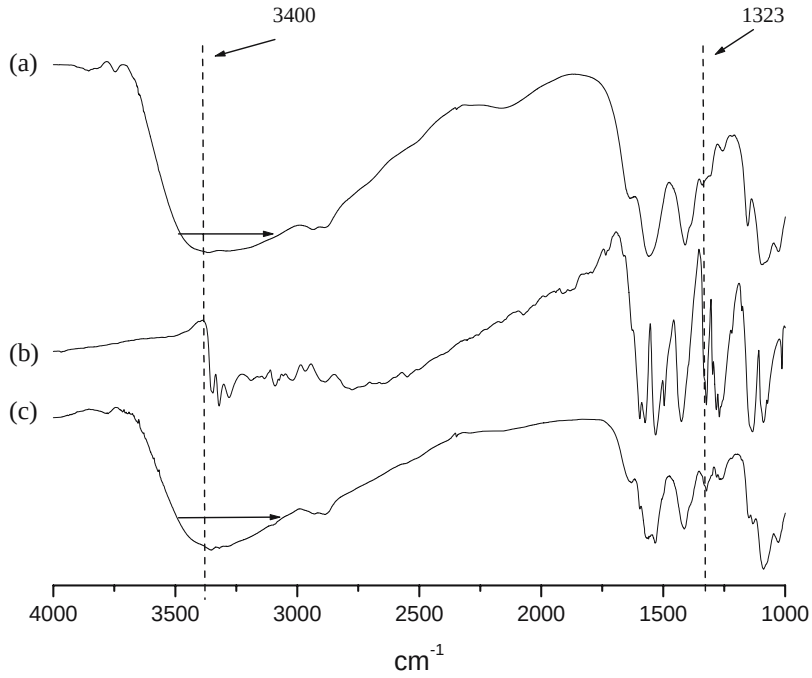

Fig. 5. FTIR spectra of (a) non-annealed chitosan template film, (b) sulfathiazole Form III crystals, and (c) sulfathiazole–chitosan solid dispersion film.

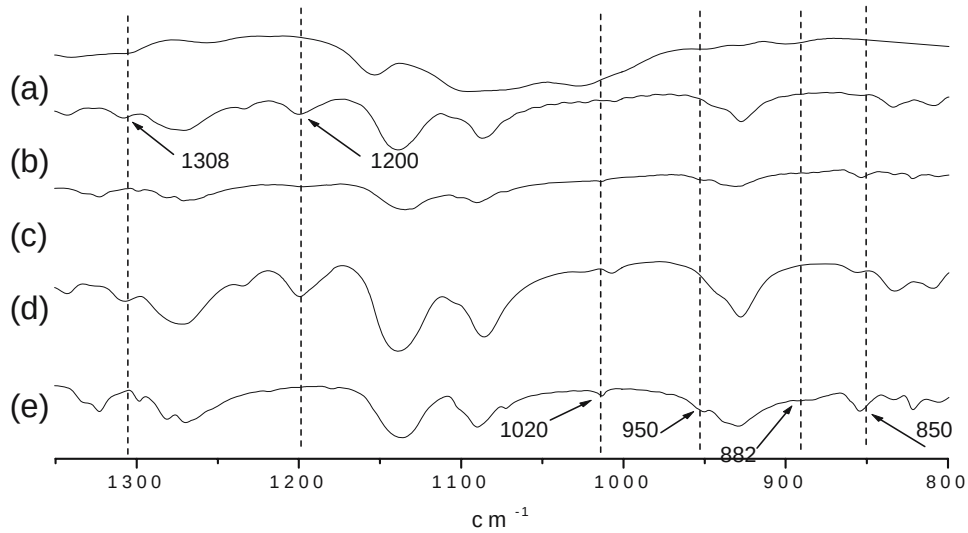

Fig. 6. FTIR spectra of the polymorphic transformation of sulfathiazole on non-annealed chitosan template films: (a) non-annealed chitosan template film, from Form I (b) to Form III (e) as the droplet volume of a saturated sulfathiazole aqueous solution increased from (b) 0.01 cm^3 to (c) 0.14 cm^3 to (d) 2.7 cm^3 and finally to (e) 20 ml at 25°C upon evaporation.

the water system with a multiple factor of 20 assuming that the solutions were ideal (36).

Since Matzger's and Myerson's methods (10,11) were water-based and evaporative, our experimental results imply that there is a need to couple other solvent screening schemes in their methods every time for screening a new polymorph of an active pharmaceutical ingredient. *Template film, droplet volume and solvent* should also play important roles in the stability of active pharmaceutical ingredients in different moist states and drying schemes such as a damped filter cake, wet granules, rotary evaporation, spray-drying, filter drying and ink-jet printing and microdroplet deposition. Interestingly, the idea of breaking up the large volume of a saturated solution into tiny volumes under the direction of templates is the underlining mechanism of biomineralization (37,38). If desired, the crystal polymorph grown on the template by Polymorph Farming on a Chip could be harvested and used as seeds for batch crystallization as well.

Although acetaminophen crystals were also grown in droplets of water and methanol under the same experimental methods as the Sulfathiazole Section, only the thermodynamically stable monoclinic Form I crystals with a melting point around 169°C by DSC (39) were obtained. Our findings was different from Matzger's result in which acetaminophen Form II was formed by water evaporation with the presence of PE-Chl. To explain our result, we must recognize that acetaminophen is a monotropic system and the melting of the orthorhombic Form II is 157°C (39) and plotted the solubility

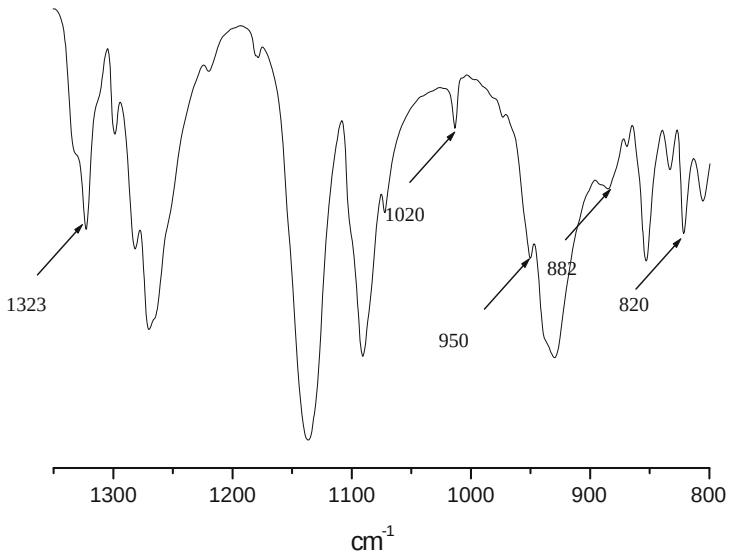

Fig. 7. The FTIR spectrum of sulfathiazole Form III crystals grown from the evaporation of a saturated methanol solution of sulfathiazole droplet with a volume of 0.01 cm^3 on a chitosan thin film. Characteristic bands for Form III were at 820, 882, 950, 1,020 and 1,323 cm^{-1}.

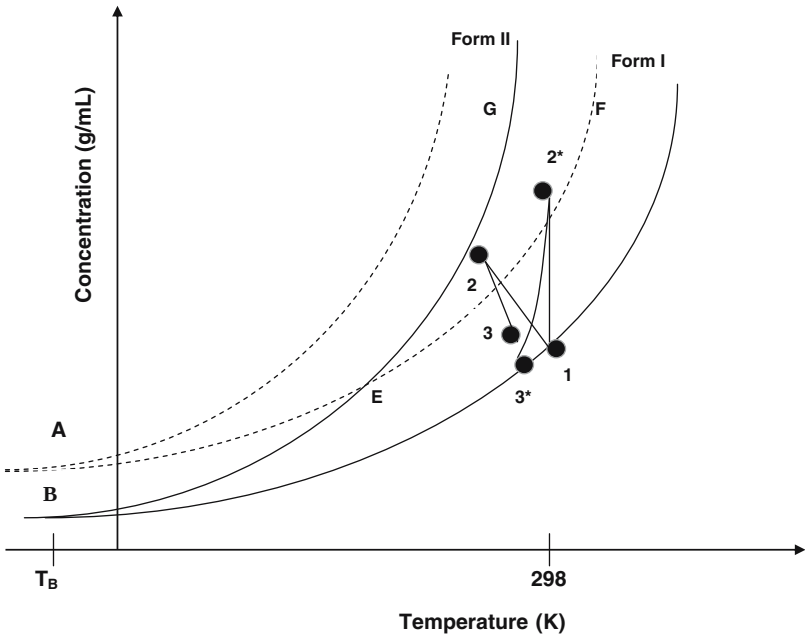

Fig. 8. Polymorphic system of two monotropically related acetaminophen Forms I and II. *Solid lines* are the solubility curves and *dash lines* are the metastable zone limits. Form transition point B at temperature T_B is below absolute zero.

curve of high melting Form I below the solubility curve of low melting Form II, so that the polymorphic transition point B lied below absolute zero (Fig. 8) (36).

Under this graphical representation, unlike sulfathiazole, the kinetically driven ABE area for acetaminophen was thought to be far below 25°C (298 K). As the initial saturated acetaminophen aqueous solution at Point 1 was evaporated, it would reach saturation and then passed through the metastable zone to either Point 2 if it was a droplet or to Point 2* if it was a 20 ml solution, at which it would spontaneously nucleate and crystallize out as Form I from Point 2 to Point 3 or from Point 2* to Point 3*. The crystalline product contained entirely of Form I throughout the whole event. *We propose* that polymorphic transformation was impossible in this thermodynamically driven delta-regime of EFG between Form I and Form II curves (36). Apparently, different pathways brought about by template films, droplet volumes and solvents could not alter the polymorphic outcome, which only depended on concentration and temperature in this case.

However, the acetaminophen crystal faces in contact with *non-annealed* PE-Chl and chitosan template films in the Interfacial Study section (Fig. 9) depend on the film materials. The amorphous nature of non-annealed and annealed chitosan and PE-Chl template films were verified by PXRD.

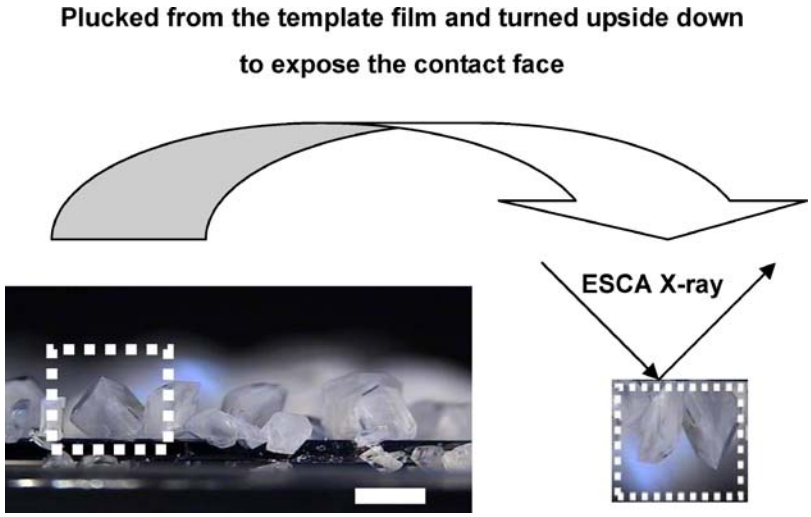

Fig. 9. A side view of acetaminophen Form I platelets grown on non-annealed PE-Chl or chitosan templates (Scale bar = 3 mm). For an ESCA analysis, the chosen crystal (*white dash box*) was picked and turned upside down so that the crystal face in contact with the template film was facing the X-ray source and detector.

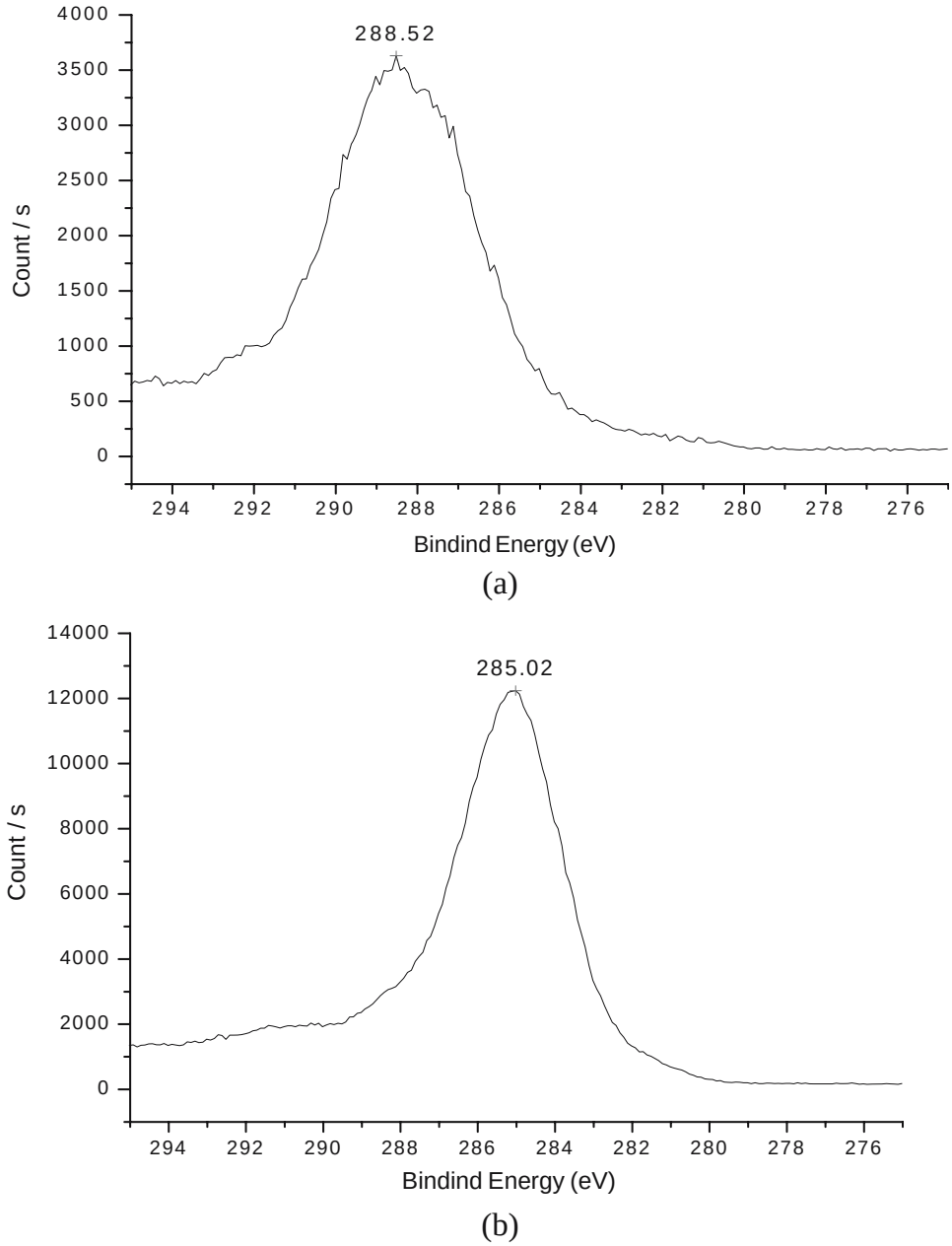

Fig. 10. (a) The crystal face in contact with a PE-Chl template showed a peak for C_{1s} at 288.5 eV which was related to the carbon on aromatic ring (C–H), and (b) The crystal face in contact with a chitosan template showed a peak for C_{1s} at 285 eV which was corresponding to the carbon on aromatic ring (C–H).

Different bonding energies for C_{1s} carbon were detected from crystal faces grown from non-annealed PE-Chl and chitosan by ESCA (Fig. 10). The shoulders in the ESCA spectra were caused by the inelastic scattering. Only those electrons emitted from the sample surface that without energy loss would be taken as photoemission peak signal. Those electrons emitted with energy loss would be taken as the scattering background or the shoulders (40). The crystal face in contact with the non-annealed PE-Chl template films showed a peak for C_{1s} at 288.5 eV and the one in contact with the non-annealed chitosan template films showed a peak for C_{1s} at 285 eV. The binding energies for C_{1s} at 285 eV and at 288–289 eV were the carbon on aromatic ring (C–H) and the carbonyl carbon (C = O) of acetaminophen, respectively (Fig. 1b) (40). Therefore, the crystal face at the non-annealed PE-Chl–acetaminophen interface was rich in carbonyl carbons (C = O) and the one at the non-annealed chitosan–acetaminophen interface was rich in aromatic carbons (C–H).

Furthermore, transmission FTIR spectra of the Molecular Interactions Study section indicated the *probable* molecular interactions between the template films and acetaminophen. Assignments of IR bands of acetaminophen, PE-Chl and chitosan are shown in Table I (32,33,41,42). Acetaminophen crystallized as a Form I phase in all solid dispersed films was supported by DSC. The transmission FTIR spectra of acetaminophen, non-annealed PE-Chl film and solid dispersed acetaminophen–PE-Chl film are shown in Fig. 11. The IR peaks at 3,163 and 1,327 cm^{-1} were due to a

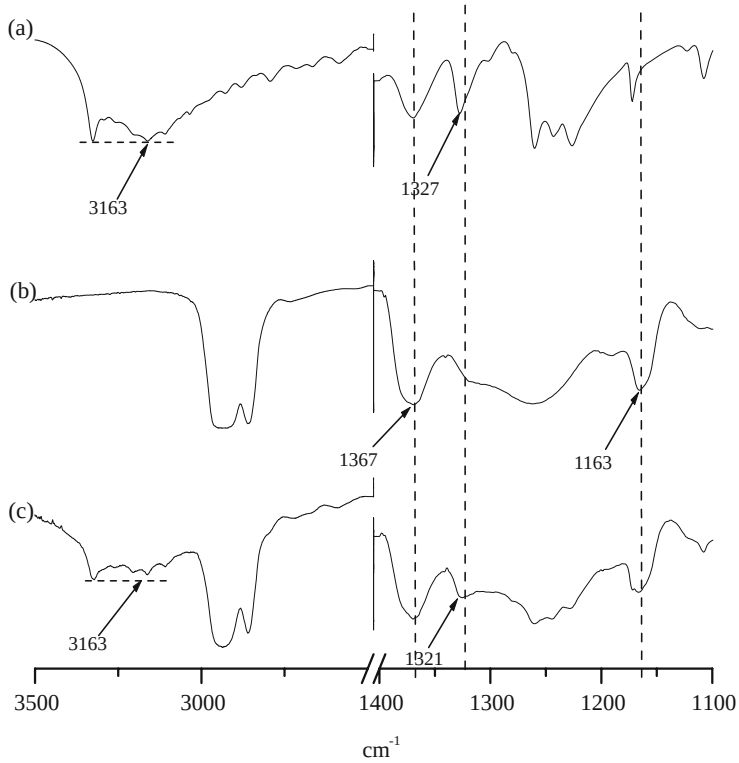

Fig. 11. The IR spectra of (a) acetaminophen, (b) PE-Ch1 film, and (c) solid dispersion film of acetaminophen and PE-Chl.

stretching vibration of –OH group of acetaminophen. But the peak at 1,327 cm^{-1} shifts to 1,321 cm^{-1} and the relative intensity of the peak at 3,163 cm^{-1} was decreased for the solid dispersed acetaminophen–PE-Chl film. This suggests that there were some interactions happening at the –OH group of acetaminophen, most likely through the hydrogen bonding between the –OH group of acetaminophen and the S = O group of PE-Chl. Although there was no detectable

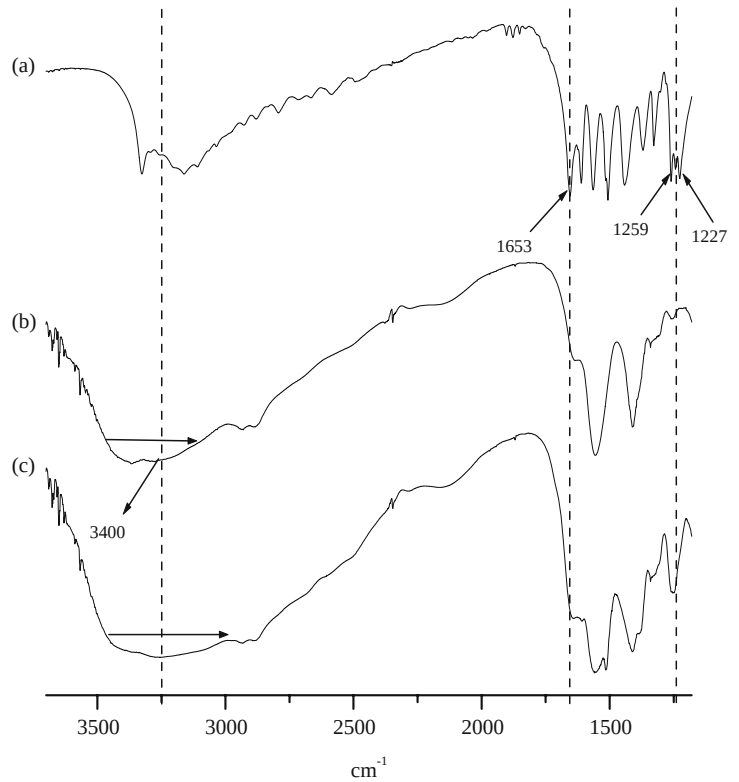

Fig. 12. The IR spectra of (a) acetaminophen, (b) chitosan film, and (c) solid dispersion film of acetaminophen and chitosan film.

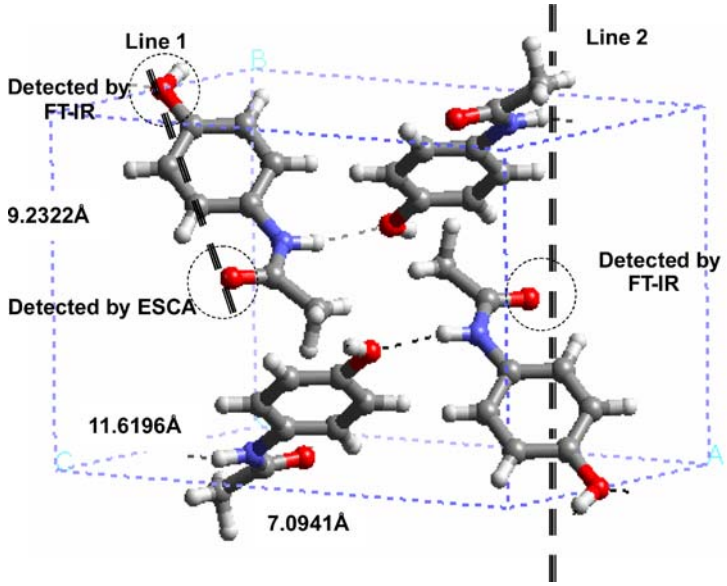

Fig. 13. The unit cell of acetaminophen monoclinic Form I: (*red*) oxygen atom and (*blue*) nitrogen atom.

change of the symmetric stretch of $–SO_2Cl–$ at 1,163 cm^{-1} and the unsymmetric stretch of $–SO_2Cl–$ at 1,367 cm^{-1} of acetaminophen–PE-Chl film due to the overlap of acetaminophen IR bands, Zheng and his co-workers illustrated that hydrogen bonding could exist between the –OH group and the –S = O group in a polymer blend (43).

The transmission FTIR spectra of acetaminophen, non-annealed chitosan film and solid dispersed acetaminophen–chitosan film are shown in Fig. 12. The peaks at 1,259, 1,227 and 1,653 cm^{-1} were the C–O, C–N, C = O stretching vibrations, respectively, of the amide group of acetaminophen (Table I). But after acetaminophen was dispersed in chitosan, these peaks disappeared or shifted and got hidden behind other peaks. The broad band around 3,400 cm^{-1} of chitosan responsible for the –OH and $–NH_2$ groups also became broader in the dispersed acetaminophen–chitosan film. These

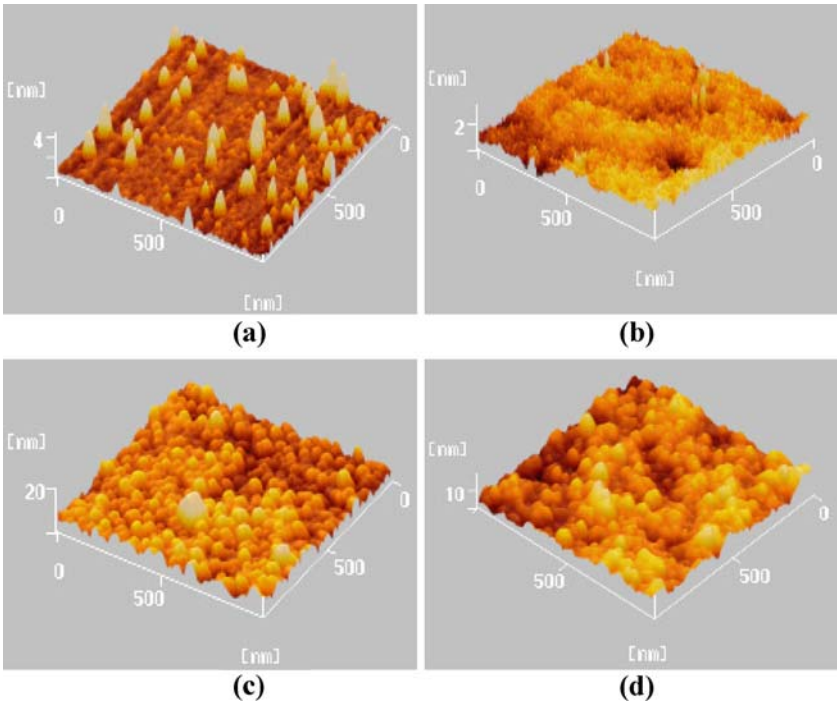

Fig. 14. AFM images of (a) a non-annealed PE-Chl template film after acetaminophen crystals were plucked, (b) an annealed PE-Chl template film which failed to grow any acetaminophen crystals, (c) a non-annealed chitosan template film after acetaminophen crystals were plucked, (d) an annealed chitosan template film which failed to grow any acetaminophen crystals.

findings suggest that there was an interaction between the C = O of acetaminophen and the primary amine $–NH_2$ of chitosan (44).

Figure 13 is a unit cell of acetaminophen Form I crystal (45). To satisfy both ESCA and FTIR spectra, we propose that Line 1 should be lying along the crystal face which was in contact with the non-annealed PE-Chl template film (Fig. 13), and Line 2 along the one which was in contact with the non-annealed chitosan template film (Fig. 13). Consequently, the crystal face containing Line 1 was anchored to PE-Chl template through the hydrogen bonding between the sulfonyl chloride $–SO_2Cl$ group with the –OH of acetaminophen. Line 1 direction was also found to be rich in the C = O groups from acetaminophen. On the other hand, the crystal face containing Line 2 was rich in aromatic carbons and the C = O was pointing perpendicularly outward to the crystal plane readily to form a hydrogen bond with the $–NH_2$ group on the other side from the chitosan template.

Although acetaminophen crystals were grown on the non-annealed PE-Chl and chitosan template films, it was not so for either the annealed PE-Chl or chitosan template thin film. AFM images in Fig. 14a and c illustrate that 50 nm particles were remained on the non-annealed PE-Chl and chitosan template film surfaces, respectively, after millimeter-sized acetaminophen crystals were plucked. These particles might well be the nuclei of a few tens of acetaminophen molecules. The number density on the PE-Chl template was about 50 nuclei/μm^2 which was greater than the one of the chitosan template of 1 nucleus/μm^2. This agrees well with the macroscopic observation that there were more crystals grown on the PE-Chl template of about 5 crystals/cm^2 (Fig. 9) than the chitosan template of less than 1 crystal/cm^2. However, such physical features were absent from the annealed PE-Chl and chitosan films as demonstrated from Fig. 14b and d, respectively. The annealing process might have changed the density, orientation and distribution of the functional groups on the template films. Figure 14 shows that it was reasonable to assume heterogeneous nucleation to be the more favorable nucleation mode when crystallization was taking place on template films.

It can be seen that Polymorph Farming on a Chip has provided a powerful technology enabling platform for crystal face study at the template-crystal interface when it was coupled with ESCA and FTIR. The molecular interactions between the template and the solute could govern the crystal face in contact with the template and they are also critical for the production of the metastable form in the solution at 25°C. Future work will be focused on the template film effect at some other temperatures.

CONCLUSIONS

Polymorph Farming on a Chip has opened up a new doorway to examine the roles of the template surface of various kinds of drug carrier, the droplet volume and the type of solvent used. The concept has been successfully demonstrated by forming thermodynamically metastable sulfathiazole Form I crystals in a small droplet volume on non-annealed chitosan templates at 25°C. With this novel method of growing crystals, FTIR was utilized to identify the polymorphism of sulfathiazole and the bonding energies for specific carbons collected by electron spectroscopy for chemical analysis (ESCA) at the acetaminophen crystal surface, together with the molecular interactions between acetaminophen and PE-Chl and between acetaminophen and chitosan in separately prepared solid dispersion film samples detected by Fourier transformed infrared (FTIR) spectroscopy, proved to be useful for identifying the crystal face of acetaminophen essential for its specific intermolecular interactions at the template-crystal interface.

ACKNOWLEDGMENTS

This work was supported by a grant from the National Science Council of Taiwan, R. O. C. (NSC 93-2119-M-008-030 and NSC 94-2119-M-008-001). Suggestions from Ms. Shew-Jen Weng in XRD and the assistance of Ms. Jui-Mei Huang in DSC and ESCA in the Precision Instrument Center and High Valued Instrument Center at National Central University are gratefully acknowledged. Suggestions from Mr. Ming-De Lu in AFM in the Department of Chemical and Materials Engineering at National Central University are appreciated.

REFERENCES

1. J. Bernstein, R. J. Davey, and J. O. Henck. Reviews: concomitant polymorphs. *Angew. Chem. Int. Ed.* **38**(23):3440–3461 (1999).
2. P. Fryer and K. Pinschower. The materials science of chocolate. *MRS Bull.* **25**(12):25–29 (2000).
3. Y. Oyumi, T. B. Brill, and A. L. Rheingold. Thermal decomposition of energetic materials. 9. Polymorphism, crystal structures and thermal decomposition of polynitroazabicyclo [3.3.1] nonanes. *J. Phys. Chem.* **90**(11):2526–2533 (1986).
4. N. Sanz, P. L. Baldeck, J. F. Nicoud, Y. FurLe, and A. Ibanez. Polymorphism and luminescence properties of CMONS organic crystals: bulk crystals and nanocrystals confined in gel-glasses. *Solid State Sci.* **3**(8):867–875 (2001).
5. K. R. Waerstad and G. H. McClellan. Preparation and characterization of some long-chain ammonium polyphosphates. *J. Agric. Food Chem.* **24**(2):412–415 (1976).
6. T. Lee and I. A. Aksay. Hierarchical structure–ferroelectricity relationships of barium titanate particles. *Cryst. Growth Des.* **1**(5):401–419 (2001).
7. A. M. Rouhi. The right stuff. *Chem. Eng. News* **Feb 24**:32–35 (2003).
8. J. Swarbrick and J. C. Boylan (eds.), *Patents in the Pharmaceutical Industry in Encyclopedia of Pharmaceutical Technology*, Vol. 11, Marcel Dekker, New York, 1995, pp. 309–328.
9. M. L. Peterson, S. L. Morissette, C. McNulty, A. Goldsweig, P. Shaw, M. LeQuesne, J. Monagle, N. Encina, J. Marchionna, A. Johnson, J. Gonzalez-Zugasti, A. V. Lemmo, S. J. Ellis, M. J. Cima, and Ö. Almarsson. Iterative high-throughput polymorphism studies on acetaminophen and an experimentally derived structure for Form III. *J. Am. Chem. Soc.* **124**(37):10958–10959 (2002).
10. M. Lang, A. L. Grzesiak, and A. J. Matzger. The use of polymer heteronuclei for crystalline polymorph selection. *J. Am. Chem. Soc.* **124**(50):14834–14835 (2002).
11. A. Y. Lee, I. S. Lee, S. S. Dette, J. Boerner, and A. S. Myerson. Crystallization on confined engineered surfaces: a method to control crystal size and generate different polymorphs. *J. Am. Chem. Soc.* **127**(43):14982–14983 (2005).
12. K. L. A. Chan and S. G. Kazarian. Fourier transform infrared imaging for high-throughput analysis of pharmaceutical formulations. *J. Com. Chem.* **7**(2):185–189 (2005).
13. Y. Fang, A. G. Frutos, and J. Lahiri. Membrane protein microarrays. *J. Am. Chem. Soc.* **124**(11):2394–2395 (2002).

14. C. A. Mitchell, L. Yu, and M. D. Ward. Selective nucleation and discovery of organic polymorphs through epitaxy with single crystal substrates. *J. Am. Chem. Soc.* **123**(44):10830–10839 (2001).
15. K. Naka and Y. Chujo. Control of crystal nucleation and growth of calcium carbonate by synthetic substrate. *Chem. Mater.* **13**(10):3245–3259 (2001).
16. P. W. Carter and M. D. Ward. Topographically directed nucleation of organic crystals on molecular single-crystal substrates. *J. Am. Chem. Soc.* **115**(3):11521–11535 (1993).
17. I. A. Aksay, T. S. Manne, I. Honma, N. Yao, L. Zhou, P. Fenter, P. M. Eisenberger, and S. M. Gruner. Biomimetic pathways for assembling inorganic thin films. *Science* **273**(5277):892–898 (1996).
18. J. F. Kang, J. Zaccaro, A. Ulman, and A. Myerson. Nucleation and growth of glycine crystals on self-assembled monolayers on gold. *Langmuir* **16**(8):3791–3796 (2000).
19. A. Sanjoh, T. Tsukihara, and S. Gorti. Surface-potential controlled si-microarray devices for heterogeneous protein crystallization screening. *J. Cryst. Growth* **232**(1–4):618–628 (2001).
20. F. Bertorelle, D. Lavabre, and S. Fery-Forgues. Dentrimer-tuned formation of luminescent organic microcrystals. *J. Am. Chem. Soc.* **125**(20):6244–6253 (2003).
21. J. E. Anderson, S. Moore, F. Tarczynski, and D. Walker. Determination of the onset of crystallization of N^1-2-(thiazolyl) sulfanilamide (Sulfathiazole) by UV–vis and calorimetry using an automated reaction platform; subsequent characterization of polymorphic forms using dispersive raman spectroscopy. *Spectrochim. Acta Part A* **57**(9):1793–1808 (2001).
22. P. D. Martino, P. Conflant, M. Drache, J. P. Huvenne, and A. M. Guyot-Hermann. Preparation and physical characterization of Forms II and III Of paracetamol. *J. Therm. Anal.* **48**(3):447–458 (1997).
23. G. Nichols and C. S. Frampton. Physicochemical characterization of the orthorhombic polymorph of paracetamol crystallized from solution. *J. Pharm. Sci.* **87**(6):684–693 (1998).
24. A. Kordikowski, T. Shekunov, and P. York. Polymorph control of sulfathiazole in critical CO_2. *Pharm. Res.***18**(5):682–688 (2001).
25. J. Anwar, S. E. Tarling, and P. Barnes. Polymorphism of sulfathiazole. *J. Pharm. Sci.* **78**(4):337–342 (1989).
26. H. Takahashi, R. Chen, H. Okamoto, and K. Danjo. Acetaminophen particle design using chitosan and a spray-drying technique. *Chem. Pharm. Bull.* **53**(1):37–41 (2005).
27. S. Zhang and K. E. Gonsalves. Chitosan–calcium carbonate composites by a biomimetic process. *Mater. Sci. Eng.* **C3**(2): 117–124 (1995).
28. H. Jiang, W. Su, S. Caracci, T. J. Bunning, T. Cooper, and W. W. Adams. Optical waveguiding and morphology of chitosan thin films. *J. Appl. Polym. Sci.* **61**(7):1163–1171 (1996).
29. S. Khoshkhoo and J. Anwar. Crystallization of polymorphs: the effect of solvent. *J. Phys. D: Appl. Phys.* **26**(8B):B90–B93 (1993).
30. J. A. Ratto, C. C. Chen, and R. B. Blumstein. Phase behavior study of chitosan/polyamide blends. *J. Appl. Polym. Sci.* **59**(9):1451–1461 (1996).
31. S. Bellú, E. Hure, M. Trapé, M. Rizzotto, E. Sutich, M. Sigrist, and V. Moreno. The interaction between mercury (II) and sulfathiazole. *Quim. Nova* **26**(2):188–192 (2003).
32. G. Saraswathy, S. Pal, C. Rose, and T. P. Sastry. A novel bio-inorganic bone implant containing deglued bone, chitosan and gelatin. *Bull. Mater. Sci.* **24**(4):415–420 (2001).
33. N. B. Colthup, L. H. Daly, and S. E. Wiberley. *Introduction to Infrared and Raman Spectroscopy* 3rd ed., Academic, New York, 1990.
34. J. L. Hilden, C. E. Reyes, M. J. Kelm, J. S. Tan, J. S. Stowell, and K. R. Morris. Capillary precipitation of a highly polymorphic organic compound. *Cryst. Growth Des.* **3**(6):921–926 (2003).
35. C. O. Bennett and J. E. Myers. *Momentum, Heat, and Mass Transfer* 3rd ed., McGraw-Hill, New York, 1982.
36. T. Threlfall. Crystallization of polymorphs: thermodynamics insight into the role of solvent. *Org. Process Res. Dev.* **4**(5): 384–390 (2000).
37. A. Veis. A window on biomineralization. *Science* **307**(5714): 1419–1420 (2005).
38. M. Hildebrand. Silicic acid transport and its control during cell wall silicification in diatoms. In E. Bäeuerlein (ed.), *Biomineralization: Progress in Biology, Molecular Biology and Application*, Wiley, Germany, 2000, pp. 159–176.
39. M. Szelagiewicz, C. Marcolli, S. Cianferani, A. P. Hard, A. Vit, A. Burkhard, M. von Raumer, U. Ch. Hofmeier, A. Zilian, E. Francotte, and R. Schenker. *In situ* characterization of polymorphic forms: the potential of raman techniques. *J. Therm. Anal. Calorim.***57**(1):23–43 (1999).
40. B. D. Ratner and D. G. Castner. Electron spectroscopyfor chemical analysis. In J. C. Vickerman (ed.), *Surface Analysis: The Principal Techniques*, Wiley, New York, 1997, pp. 50–58.
41. S. L. Wang, S. Y. Lin, and Y. S. Wei. Transformation of metastable forms of acetaminophen studied by thermal fourier transform infrared (FT-IR) microspectroscopy. *Chem. Pharm. Bull.* **50**(2):153–156 (2002).
42. A. Roychoudhury and P. P. De. Studies on chemical interactions between chlorosulphonated polyethylene and carboxylated nitrile rubber. *J. Appl. Polym. Sci.* **63**(13):1761–1768 (1996).
43. H. Lu, S. Zheng, B. Zheng, and X. Tang. Miscibility and intermolecular specific interactions in blends of poly(hydroxyether sulfone) and poly(*N*-vinylpyrrolidone). *Macromol. Chem. Phys.* **205**(6):834–842 (2004).
44. H. Takahashi, R. Chen, H. Okamoto, and K. Danjo. Acetaminophen particle design using chitosan and a spray-drying technique. *Chem. Pharm. Bull.* **53**(1):37–41 (2005).
45. www.accelrys.com. C^2 Polymorph. Cerius^2 Datasheet.